

A Fast Aerodynamic Procedure for a Complete Aircraft Design Using the Know Airfoil Characteristics

Luiz Augusto Tavares de Vargas

Federal University of Minas Gerais, Center for Aeronautical Studies.

Paulo Henriques Iscold Andrade de Oliveira

Federal University of Minas Gerais, Center for Aeronautical Studies.

Copyright © 2006 Society of Automotive Engineers, Inc

ABSTRACT

The performance and flight characteristics of an aircraft are markedly affected by the aerodynamic design, which can be done making use of various tools such as wind tunnel tests and computer simulations. Despite the fact that wind tunnel testing permits great trustworthiness of results, they are still slow and costly procedures. On the other hand, computational methods allow for faster and lower budget analysis. For the conception and the initial phase of an aircraft design, where it is necessary to evaluate a great variety of wings and lifting surfaces configurations, it is desirable to have a method able to determine the main aerodynamic characteristics, such as drag and lift, quickly. In more advanced phases of the design the interest is in obtaining results which shows a more detailed flow around the aircraft. This paper describes a fast method with good results for the calculation of aerodynamic characteristics of a complete aircraft where a simple three-dimensional numeric model is corrected based on the characteristics of bi-dimensional flow around the aerodynamic profile experimentally obtained, with an option of adding to the method a free wake model and measurement of induced drag through the *Momentum* variation. This procedure results in a non linear method capable of predicting lift, induced drag, parasite drag, aerodynamic moments both in linear regions as well as stall regions in the lift curve of a complete aircraft, including effects due to yaw, pitch and roll, and the influence between surfaces. This paper presents some results obtained with this procedure and compares them to experimental results.

INTRODUCTION

In initial phases of design activities, the detailed knowledge of all the flow around the aircraft is not relevant, the designer is interested only in the resulting aerodynamic forces (drag, lift and moments), which motivate the development of diverse specific techniques for

determination of these aerodynamic forces, without the need for solution of the entire flow camp (Boundary Element Method), highlighting the methods: Lifting Line (Prandtl, 1921), Vortex-Lattice (Lamar, 1976) and Panels (Hess and Smith, 1966).

Since the objective of this paper regards design activities for complete aircrafts and related work, an analysis procedure is considered efficient when, aside from supplying coherent results in comparison with experimental measurements, it is also robust and fast, as well as applicable to a great variety of cases. The condition of necessity of applicability to multiple lifting surfaces of complex geometries makes it impossible to use the Classic Lifting Line method, while the condition of processing speed makes it impossible to use the panel method, which makes the Vortex-Lattice method the natural choice.

THE CLASSICAL METHOD

The Vortex-Lattice method is based on the solution of the Laplace equation through the distribution of singularities (horseshoe vortex) along the body, which responds to the condition of impermeability (flow cannot pass throughout a non-porous surface).

In its classic formulation, the vortex-lattice method has singularity distributions both along the span as well as in the camber line of the airfoil. However, in the proposed method, since bi-dimensional information on the aerodynamic airfoil would be used, the distribution along the chord becomes unnecessary. This method is also known as Weissinger (Weissinger, 1947), or modern lifting line (Phillips and Snyder, 2000). The distribution of bounded vortex is at every $\frac{1}{4}$ of chord, and the control points are at $\frac{3}{4}$ of chord, satisfying the Kutta's condition in the trailing edge, as seen in Figure 1.

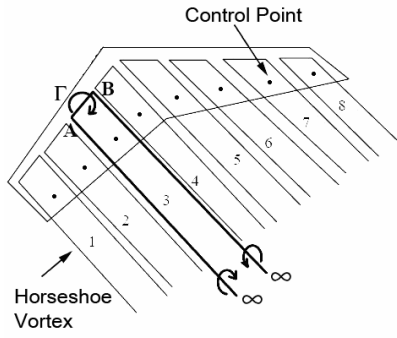


Figure 1. Distribution of vortex in the Weissinger method

Instead of using the classic flat horseshoe vortex, a more interesting form is shown in Figure 2, in which the horseshoe vortex is composed by discrete vortex segments which, follows the surface until the trailing edge and then align to the free stream (Miranda, Elliott, Baker, 1977). This method can be modified to include a free wake and unsteady aerodynamic models.

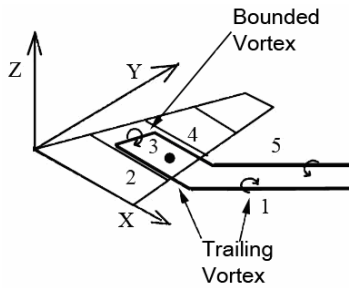


Figure 2. Adopted vortex system

The solution of the Vortex-Lattice model is based on a development of the Bio-Savant theorem (Katz and Plotkin, 1991). The speed in point P induced by a straight vortex line segment that goes from point A to point B, as shown in Figure 3, can be calculated through the Eq. (1).

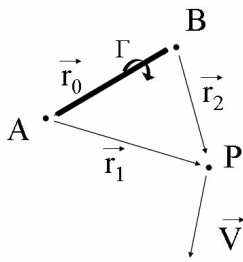


Figure 3. Velocity induced by a straight vortex line segment

$$\vec{V} = \frac{\Gamma}{4\pi} \frac{\vec{r}_1 \times \vec{r}_2}{|\vec{r}_1 \times \vec{r}_2|^2} \vec{r}_0 \cdot \left(\frac{\vec{r}_1}{|\vec{r}_1|} - \frac{\vec{r}_2}{|\vec{r}_2|} \right) \quad (1)$$

Where \vec{V} denotes the speed induced by a vortex segment, Γ denotes the intensity of the vortex and \vec{r}_0 to \vec{r}_2 are the distances indicated in Figure 3.

The solution of the potential flow problem will be the determination of the intensities Γ of each horseshoe vortex through a system of linear equations as shown in Eq.(2), with the boundary condition being the condition of body impermeability.

$$\begin{bmatrix} w_{11} & w_{12} & \cdots & w_{1n} \\ w_{21} & w_{22} & \cdots & w_{2n} \\ \vdots & \vdots & \vdots & \vdots \\ w_{m1} & w_{m2} & \cdots & w_{mn} \end{bmatrix} \times \begin{Bmatrix} \Gamma_1 \\ \Gamma_2 \\ \vdots \\ \Gamma_n \end{Bmatrix} = \begin{Bmatrix} B_1 \\ B_2 \\ \vdots \\ B_n \end{Bmatrix} \quad (2)$$

Where w denotes the geometric influence on normal induced speed on the panel m by the horseshoe vortex n , Γ_n denotes the intensity of the horseshoe vortex n and B denotes the speed of normal free flow at the panel surface in the control points, including the components due to maneuver (rolling, pitch and yaw).

Once the intensity of each horseshoe vortex is determined, the aerodynamic forces can be calculated according to the Kutta-Joukowski theorem as show in Eq. (3) (Katz and Plotkin, 1991) resulting in the distribution of force, in each panel, as shown in Figure 4.

$$\vec{F} = \rho \vec{V} \times \vec{\Gamma} \quad (3)$$

Where \vec{F} denotes the resulting force at $1/4$ of the chord, ρ the fluid density, \vec{V} the resulting vector for the speed at $1/4$ of chord and $\vec{\Gamma}$ the bounded vortex.

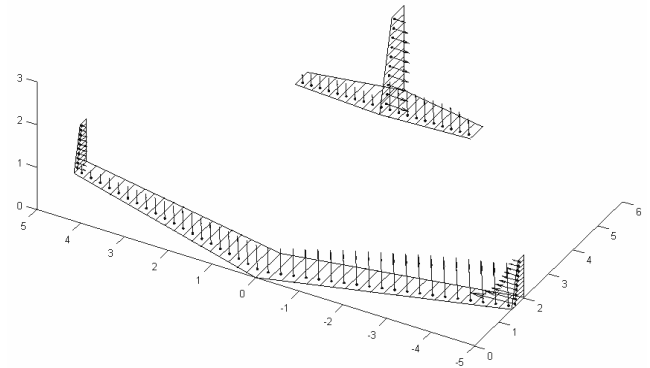


Figure 4. Distribution of acting forces on the aircraft

NON LINEARITY

Since the distribution of horseshoe vortex occurs only along the span, with only one control point along the chord disregarding the line of camber of the airfoil, the results obtained with the traditional method refer to a wing that

uses a symmetric aerodynamic profile, which, according to the linear theory is equivalent to a flat plate, with a lift slope ($dCL/d\alpha$), constant equal to 2π and the null lift angle (α_0) constant and equal to zero.

In order to avoid this problem and correct the three-dimensional results of flow obtained with the flat plate as a function of aerodynamic characteristics of the real airfoil, an iterative process based on the method proposed by Mukherjee and Gopalathnam (Mukherjee and Gopalathnam, 2003) will be used.

This iterative algorithm is capable of computing the influence of bi-dimensional flow characteristics on three-dimensional flow and can be described through the following steps:

(1) Initial values of δ and ΔC_L are assumed for each section of the wing.

(2) The aerodynamic characteristics are calculated using the traditional Vortex-Lattice algorithm

(3) The effective attack angles for each section (α_{e_sec}) are calculated using the local lift value obtained in step (2) using the equation 1.4

$$\alpha_{e_sec} = \frac{C_{L_{sec}}}{2\pi} - \delta \quad (4)$$

(4) The value of $\Delta C_L = C_{L_{visc}} - C_{L_{sec}}$, is calculated, where $C_{L_{sec}}$ is the value obtained with the conventional Vortex-Lattice method, and $C_{L_{visc}}$ is the value obtained using the information of the airfoil and effective attack angles for each section of the span (bi-dimensional polar curves).

(5) The new value of δ is calculated using Eq. (5) and the new angle of attack of which sections became the initial angle of attack plus the new value of δ , as show in Eq. (6).

$$\delta = \delta + \frac{\Delta C_L}{2\pi} \quad (5)$$

$$\alpha_{sec} = \alpha_{initial} + \delta \quad (6)$$

(6) Return to (2), where α_{sec} is the new value for the attack angle of each section to be used for the calculation with the traditional method. This process is repeated until $C_{L_{sec}}$ converges.

When the effective attack angle for each station and the profile polar is known, beyond getting the lift

coefficient, it is possible to obtain the drag parasite and aerodynamic moment coefficients for each wing section.

Mukherjee and Gopalathnam, tested the algorithm only in individual wings in simple flight conditions (without roll, pitch and yaw velocities); however, in this paper, this method was used successfully in complete aircrafts with complex geometries and maneuvering conditions.

However, in order to use the algorithm in a complete aircraft with multiple wings and tails with complex geometries and in flight conditions with movements such as roll, pitch and yaw, it was necessary to use a dumping and dissipation coefficient, which are not included in the original algorithm suggested by Mukherjee and Gopalathnam, which brings more stability to the numeric method, transforming the Eq. (5) into the form shown (7) and (8).

$$\delta_i = \delta_i + \frac{1}{K+1} \frac{\Delta C_L}{2\pi} \quad (7)$$

$$\delta_i = \frac{\left(\delta_i + \Pi \frac{(\delta_{i-1} + \delta_{i+1})}{2} \right)}{1 + \Pi} \quad (8)$$

Where i denotes the section throughout the span, K is the dumping factor and Π is the dissipation factor.

THE INDUCED DRAG

Because the difficulties associated with the calculation of the induced drag present in a lifting surface, there is many ways to estimate it, such the backward component of force calculated with the Kutta-Joukowski theorem (Eq.(3)), a modified Lifting Line method proposed by Eppler which computes the downwash in the trailing edge, and pressure integration (Mortara, Strausfogel, Maughmer, 1992).

A more accurate way to estimate induced drag given by Kutta-Joukowski theorem is measuring the variation of kinetic energy (*Momentum*) in a plane behind the aircraft (Giles, M. B. and Cummings R. M., 1999), because its valid for any kind of wing geometry and multiple surfaces even for a complete aircraft including the fuselage (as show in Jie, Fengwei and Qin, 2003).

The variation of *Momentum* in the perpendicular direction to free stream in the Area S_6 of Figure 5 is the drag caused by the aircraft and can be computed with the Eq.(9). This technique is known as far field or Trefftz-Plane analysis.

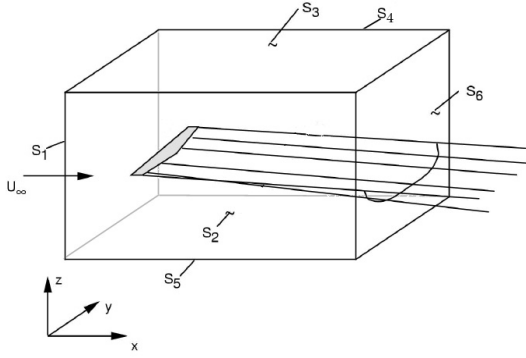


Figure 5. Control volume used to measure induced drag.

$$D_{IND} = \frac{1}{2} \rho \int_{-\infty}^{\infty} \int_{-\infty}^{\infty} (v^2 + w^2) dy dz \quad (9)$$

However, a more convenient way of treating the Eq. (9) is obtained using the Green theorem (Katz and Plotkin, 1991) which converts an area integral into a line integral, and the induced drag equation assumes the form presented in Eq. (10).

$$D_{IND} = \frac{1}{2} \rho \int_{-b/2}^{b/2} \Delta\phi \cdot W_p ds \quad (10)$$

Where $\Delta\phi$ denotes the difference of potential between the top and the bottom side of the wake, and W_p is the normal flow speed in thought the wake.

As in the method of horseshoe vortex distribution, the difference in potential in the wake is the circulation ($\Delta\phi = \Gamma$), and the induced drag could be conveniently calculated through the Eq.(11).

$$D_{IND} = \frac{1}{2} \rho \sum_{i=1}^n \Gamma_i W_{pi} s_i \quad (11)$$

Where D_{IND} denotes the induced drag, ρ denotes the density of the fluid, Γ the intensity of the horseshoe vortex, W_p the normal induced velocity through the wake and s the width of the horseshoe vortex. All of these values are measured in points distant of the wing as shown in Figure 6. This formulation is also valid for any wake form, even for the rolled-up vortex sheet (Schlichting, H.; Truchenbrodt, 1979).

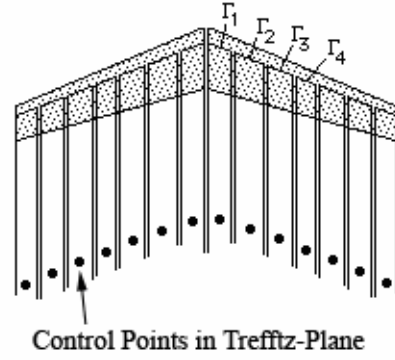


Figure 6. Calculation points used to measure the induced drag in Trefftz-Plane

FREE WAKE

The alignment of the horseshoe vortex with the free wake, as described previously (Figure 2), is a good approximation for the calculation of fixed wing aircrafts in less severe flight conditions (no maneuvers), since the geometry of the wake has little influence in the aerodynamic results of interest (lift and drag coefficients) of the surface which generated it in steady flow.

However, when a more complex geometry of wing and maneuver conditions in which the wake passes very close to a lift surface, such as, for example, the tail in the trajectory of the wing wake, as shown in Figure 7, the precise calculation of the geometry of the wake can affect the result in some flight conditions and, unsteady flow (Katz and Maskew, 1987).

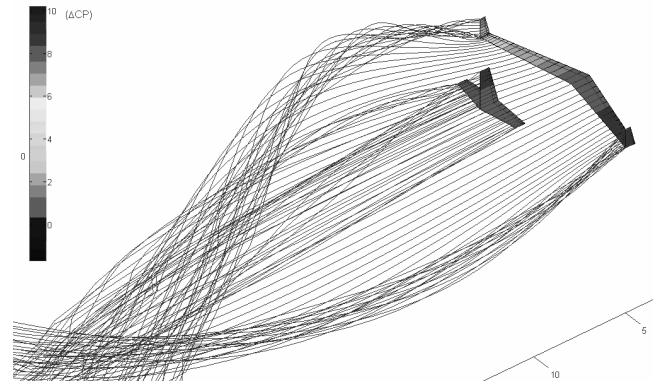


Figure 7. Result of Differential Pressure using a model of free wake during a roll maneuver around the traction line.

In order to solve this problem, a free wake model can be added to the Vortex-Lattice model. This is a non linear and transient iterative process which demands long processing time, since the wake is discretized in distinct elements and the horseshoe vortex trajectory is calculated.

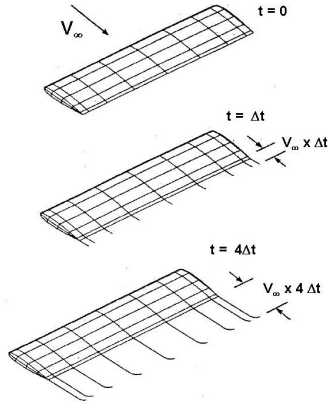


Figure 8. Evolution of the stream line and the trailing vortex

The algorithm used for the calculation of the free wake is based on the ideas proposed by Katz and Maskew (Katz and Maskew, 1987) and can be described as following:

(1) Entrance of the initial geometry of the horseshoe vortex where the trailing vortex extends on the surface of the body from the bonded vortex ($1/4$ of chord) to the trailing edge only (instant $t = 0$ in Figure 8).

(2) The vortex-lattice method is used in order to calculate the intensity of the vortex and the velocity in the control points of the wake.

(3) With the velocities in the control points, the trajectory of a fluid particle located on these points is calculated (stream lines) using a numerical integrator, as shown in equations (12) and (13).

$$(x, y, z)_{t_0+\Delta t} = (x, y, z)_{t_0} + (\Delta x, \Delta y, \Delta z) \quad (12)$$

Where:

$$(\Delta x, \Delta y, \Delta z) = (u, v, w)\Delta t \quad (13)$$

(3) The trailing vortex is then extended over the calculated fluid particle trajectory (stream line).

(4) Return to (2), until the convergence criteria adopted or a pre-established number of iterations is obtained.

It is important to note that this is an elliptic problem, in other words, it is necessary to re-calculate the entire wake at each iteration, since the most distant vortex segment of the wing modifies the beginning of development of the wake, closest to the wing.

It is also important to highlight that in step (3), the equations (12) and (13) refer to a first order integrator (Euler). It is advisable to use a numeric integrator of

superior order, such as the Runge-Kutta of second or fourth order, which improves the precision of results.

RESULTS

Two configurations frequently used in light aircraft are rectangular and tapered wings, so these have been chosen to demonstrate the applicability of the proposed method, taking into consideration that both wings are constituted by the aerodynamic airfoil NACA 0012, for which the aerodynamic coefficient curves considered can be seen in Figure 9.

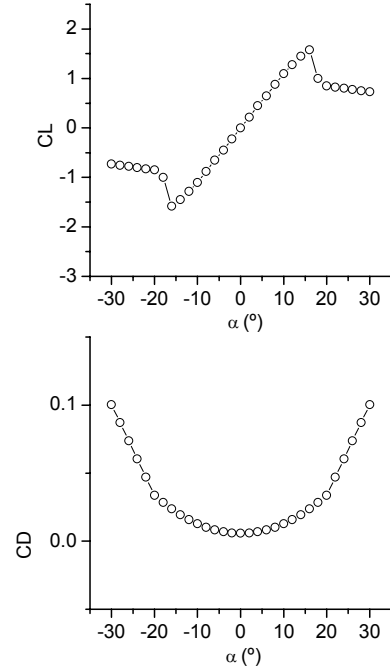


Figure 9. Aerodynamic characteristics considered for the NACA 0012 airfoil

The choice in using the NACA 0012 airfoil as an example in the application of the method is due to the fact that it has a symmetric airfoil, with the same aerodynamic characteristic as a flat plate in the traditional vortex-lattice method, which makes it possible to make direct comparisons between the results obtained linearly and non linearly, using the information on the bi-dimensional profile.

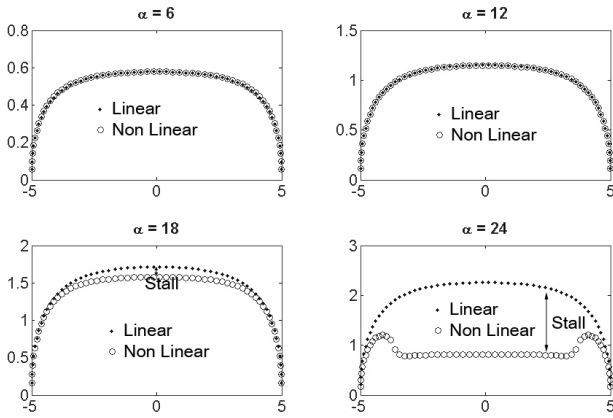


Figure 10. Distribution of CL in a typical rectangular wing.

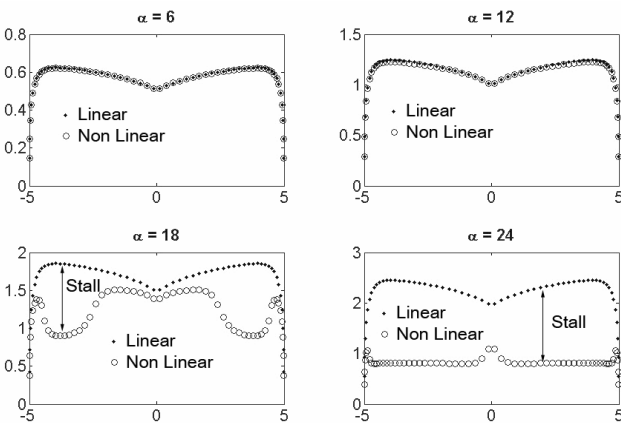


Figure 11. Distribution of CL in a typical trapezoidal wing.

The results of the distribution of the lift coefficient for both wings in diverse attack angles can be seen in Figure 10 and Figure 11, where one can note the occurrence of stall in elevated attack angles. Such a prediction is possible thanks to the use of the bi-dimensional profile information, while, according to the traditional method, the wing would continue to afford lift.

Figure 12 and Figure 13 shows the respective lift and drag curves obtained with the proposed method, compared with the classical linear method, where can be noted the good prediction of the stall with the non linear method, while with the liner method the wing always continue lifting.

An example of applicability of the method in asymmetric profiles can be seen in Figure 14, in which the results obtained numerically for various rectangular wings with diverse aspect ratios are compared to experimental results (Mukherjee and Gopalathnam, 2006). As can be seen the present method presents good results, compatible with the experimental results even for the post-stall region of the lift curve.

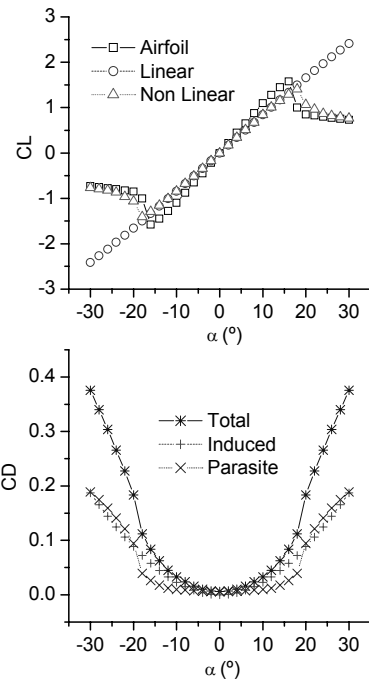


Figure 12. Aerodynamics coefficients of a rectangular wing obtained with the implemented software

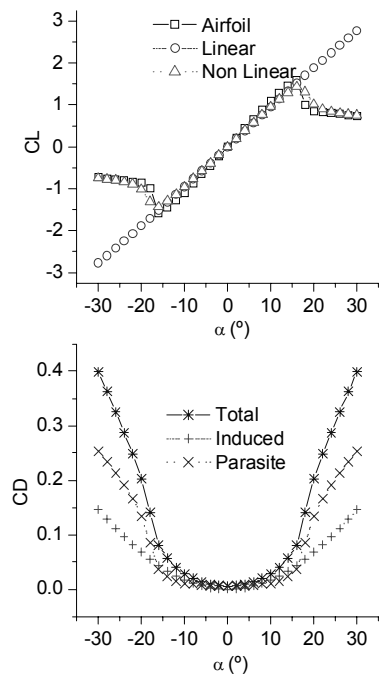


Figure 13. Aerodynamics coefficients of a trapezoidal wing obtained with the implemented software.

For analysis of the influence of the wake geometry in aerodynamic coefficients, a critical case has been chosen, which a Canard wing configuration is, because the canard's tip vortex of pass through the main wing in the maximum lift region along the span, so the precise calculus of the wake should affect the results.

It is interesting to notice that even in this configuration, the geometry of the wake have a discrete influence on the aircraft aerodynamic coefficients, as can be seen in Figure 15, where the results obtained with the free wake model are compared to the classic horseshoe vortex, in which the trailing vortex is fixed and not aligned to the free stream (as show in Figure 1), and the horseshoe vortex, in which the trailing vortex is fixed and aligned to free flow (as show in Figure 2).

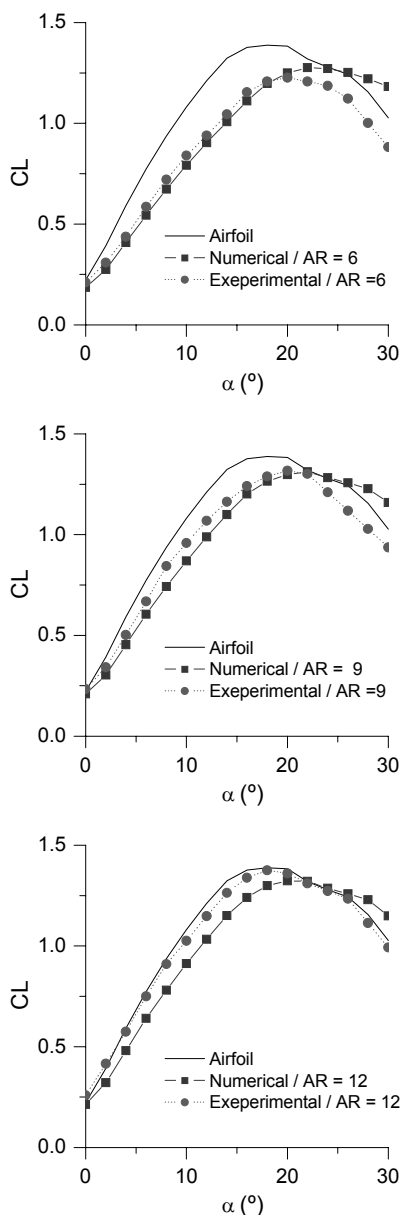


Figure 14. Polar curves obtained numerically and experimentally for some rectangular wings, using the NACA 4415 profile.

As show in Figure 15, in general, for fixed wings aircrafts, the free wake model has a little influence in the polar of the aircraft and just a flat wake with trailing vortex aligned with the free stream is sufficient to assure good

results in most of cases. However, for specific cases such as high angular speeds during the aircraft maneuver or a rotor blade, as shown in 7, the free wake model must be used (Leishman, J. G.; Bhagwat, M. J. and Bagai, A., 2002).

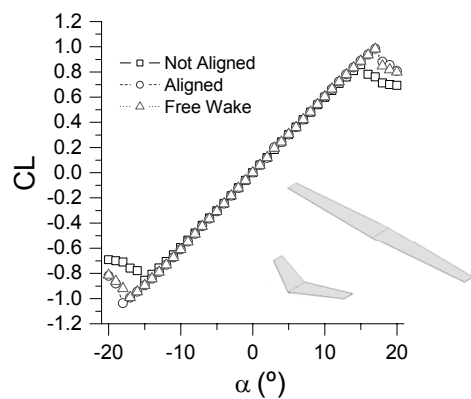


Figure 15. Polar curves obtained with different wake geometries for a canard configuration

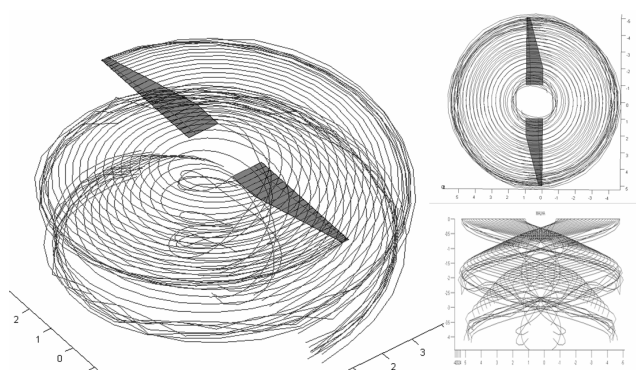


Figure 16. Wake generated by a rotor blade

ADVANTAGE OF THE METHOD

- Use of available bi-dimensional information of the aerodynamic profile, obtained experimentally or calculated numerically, thus being able to calculate the non linear region of the lift curve (stall), include parasite drag effects and aerodynamic moment.
- Make it possible to use complex geometries with infinite planar and non-planar surfaces, including geometric torsion, dihedral and sweep.
- Allows aerodynamic torsion with different airfoil at root and tip of surfaces.
- Any kind of mesh distribution can be used, with four types available at this implementation.
- Calculation of forces, moments and their respective coefficients in three different

coordinate systems (body axis, stability axis and wind axis).

- Aligned or not Aligned flat fix wake
- Additional model of free wake
- Calculation of induced drag using the Trefftz-Plane model
- Allows for diverse flight conditions including the incidence angle known as β , and maneuvers (roll, pitch and yaw).
- Great processing speed, making use of approximately 2 seconds for a complete aircraft analysis composed of 100 panels, including processing and graphic result (obtained in a PC, 1.4 GHz, and 512 MB of RAM).
- Can incorporate a panel method for the fuselage

CONCLUSIONS

The methodology described in this paper is of great value for the design of complete aircrafts, meeting the needs for initial and less detailed phases, as well as phases which call for greater detail for the aircraft.

This methodology can be extended to other areas of aerodynamics such as the design of blades and propellers due to the free wake model.

It can also be used in conjunction with a flight simulator, since, due to its great processing speed, for a reduced number of panels (in flight simulators, precision can be smaller) the processing is almost immediate, substituting pre-established aerodynamic characteristics with values calculated in real time.

For more real results for a complete aircrafts a fuselage model with panel method must be done.

REFERENCES

- [1] Anderson J. D.; "Fundamentals of Aerodynamics", McGraw-Hill, Inc; 2° ED, 1991.
- [2] Giles, M. B. and Cummings R. M., "Wake Integration for Three-Dimensional Flowfield Computations: Theoretical Development", Journal of Aircraft, vol.36, n° 2, 1999.
- [3] Hess J. L.; Smith A. M. O., "Calculation of Potential flow about arbitrary bodies", Douglas Aircraft Company, Aircraft Division, Long Beach, California, 1966.
- [4] Katz, J.; Maskew, B.; "Unsteady Low-Speed Aerodynamic Model for Complete Aircraft Configurations"; Journal of Aircraft, vol.25, n° 4 , 1987.
- [5] Katz, J.; Plotkin, A.; "Low - Speed Aerodynamics: From wing Theory to Panel Methods", McGraw-Hill, Inc, 1991.
- [6] Jie, L.; Fengwei ,L.; Qin, E;" Far-Field Drag-Prediction Technique Applied to wing Design for Civil Aircraft"; Journal of Aircraft, vol.40, n° 3, 1999.
- [7] Lamar, J., E, "A Vortex-Lattice Method for the Mean Camber Shapes of Trimmed Noncoplanar Planforms with Minimum Vortex Drag", NASA TN D-8090, 1976.
- [8] Leishman, J. G.; Bhagwat, M. J. ; Bagai, A.; " Free-Vortex Filament Methods for the Analysis of Rotor Wakes"; Journal of Aircraft, vol.39, n° 5, 2002.
- [9] Miranda, L. R.; Elliott R. D.; Baker, W. M.;" A Generalized Vortex Lattice Method for Subsonic and Supersonic Flow Applications", NASA CR 2865, 1977.
- [10]Mortara K.W.; Straussfogel D. M.; Maughmer, M.D.; "Analysis and Design of Planar and Non-Planar Wings for Induced Drag Minimization, NASA-CR-191274, 1992.
- [11]Mukherjee, R.;Gopalarathnam, A.; Kim S. "An Iterative Decambering Approach for Post-Stall Prediction of Wing Characteristics from Known Section Data"; 41st Aerospace Sciences Meeting and Exhibit, Reno, Nevada, 6-9 de Janeiro, 2003.
- [12]Mukherjee, R.;Gopalarathnam, A.; Kim S. "Poststall Prediction of Multiple-Lifting-Surface Configuration Using a Decambering Approach"; Journal of Aircraft, vol.43, n° 3 , 2006.
- [13]Phillips, W. F.; Snyder D. O.; "Modern Adaptation of Prandtl's Lifting-Line Theory"; Journal of Aircraft, vol.37, n° 4 , July- August 2000.
- [14]Prandtl, L. " Applications of modern hydrodynamics to aeronautics"; NACA-116, 1921
- [15]Schlichting, H.; Truchenbrodt, E.; Ramm, H. J. "Aerodynamics of the Airplane"; McGraw-Hill, 1979.
- [16]Weissinger J. "The Lift Distribution of Swept-back Wings", Technical Memorandum n° 1120, NACA, Washington, 1947.